ARTICLE

BIOTECHNOLOGY and BIOENGINEERING

A High Gas Fraction, Reduced Power, Syngas Bioprocessing Method Demonstrated With a *Clostridium ljungdahlii* OTA1 Paper Biocomposite

Mark J. Schulte,[1] Jeff Wiltgen,[1] John Ritter,[1] Charles B. Mooney,[2] Michael C. Flickinger[1,3]

[1]Department of Chemical and Biomolecular Engineering, North Carolina State University, 911 Partners Way, Raleigh, North Carolina 27695

[2]Analytical Instrumentation Facility, North Carolina State University, Raleigh, North Carolina

[3]Golden-LEAF Biomanufacturing Training and Education Center, North Carolina State University, Raleigh, North Carolina 27695; telephone: +1-919-515-0175; fax: +1-919-513-8235; e-mail: michael_flickinger@ncsu.edu

ABSTRACT: We propose a novel approach to continuous bioprocessing of gases. A miniaturized, coated-paper strip, high gas fraction, biocomposite absorber has been developed using slowly shaken horizontal anaerobic tubes. Concentrated *Clostridium ljungdahlii* OTA1 was used as a model system. These gas absorbers demonstrate elevated CO mass transfer with low power input, reduced liquid requirements, elevated substrate consumption, and increased product secretion compared to shaken suspended cells. Concentrated OTA1 cell paste was coated by extrusion onto chromatography paper. The immobilized system shows high, constant reactivity immediately upon rehydration. Cell adhesion was by adsorption to the cellulose fibers; visualized by SEM. The *C. ljungdahlii* OTA1 coated paper mounted above the liquid level absorbs CO and H_2 from a model syngas secreting acetate with minimal ethanol. At 100 rpm shaking speed (7.7 Wm^{-3}) the optimal cell loading is 6.5 $g_{DCW}\,m^{-2}$ to maintain high CO absorbing reactivity without the cells coming off of the paper into the liquid phase. Reducing the medium volume from 10 mL to 4 mL (15% of tube volume) did not decrease CO reactivity. The reduced liquid volume increased secreted product concentration by 80%. The specific CO consumption by paper biocomposites was higher at all shaking frequencies <100 rpm than suspended cells under identical incubation conditions. At 25 rpm the biocomposite outperforms suspended cells for CO absorption by 2.5-fold, with an estimated power reduction of 97% over the power input at 100 rpm. The estimated minimum k_La for miniaturized biocomposite gas-absorbers is ~100 h^{-1}, *10 to 10^4 less power input* than other syngas fermentation systems reported in the literature at similar k_La. Specific consumption rates in a biocomposite were ~14 mmol $g_{DCW}^{-1}\,h^{-1}$. This work intensified CO absorption and reactivity by 14-fold to 94 mmol CO $m^{-2}\,h^{-1}$ over previous *C. ljungdahlii* OTA1 work by our group. Specific acetate production rates were 23 mM h^{-1} or 46 mmol $m^{-2}\,h^{-1}$. The specific rates and apparent k_La scaled linearly with biocomposite coating area.

Biotechnol. Bioeng. 2016;9999: 1–11.

KEYWORDS: *Clostridium ljungdahlii*; gas-to-liquid fuels; biocomposite; process intensification; biofuels; syngas

Introduction

Gas-to-liquid (GTL) biocatalysis is attractive for carbon recycling with production of fuels and chemicals because of substrate flexibility, product specificity, and mild reaction conditions (Buchholz, 2012). Genetic engineering of gaseous carbon assimilating microorganisms to produce different products is currently being intensely investigated (Drzyzga et al., 2015). However, GTL biocatalysis is limited by the energy cost for dispersion of low solubility gases into aqueous media, slow volumetric substrate consumption, slow specific production rates, and low product titers (Abubackar et al., 2011; Bengelsdorf et al., 2013; Drzyzga et al., 2015; Wilkins and Atiyeh, 2011).

These limitations are particularly evident in stirred tank bioreactors (STRs) which consume a substantial amount of energy to contact low solubility gases with suspended cells (1,000–10,000 $W\,m^{-3}$). The power required to disperse large volumes of gas into a large liquid phase increases operating costs. In the absence of cell recycle, this limits the cell density and therefore gas consumption/product production rate achievable with STRs at large scale. These systems are often not continuous processes. As a

Correspondence to: M.C. Flickinger
Contract grant sponsor: North Carolina Biotechnology Center (NCBC)
Contract grant sponsor: National Institutes of Health Molecular Biotechnology Training Program
Contract grant number: T32 GM008776-11
Contract grant sponsor: Golden LEAF Biotechnology Training and Education Center (BTEC)
Received 16 November 2015; Revision received 2 February 2016; Accepted 21 February 2016
Accepted manuscript online xx Month 2016;
Article first published online in Wiley Online Library (wileyonlinelibrary.com).
DOI 10.1002/bit.25966

result, cell concentrations are low, mass transfer resistance can be significant, the secreted products may accumulate to toxic levels, and specific production rates are low compared to sugar substrate fermentations which can achieve production rates of $>10\,g\,L^{-1}\,h^{-1}$ ($>200\,mM\ h^{-1}$) (Bayrock and Ingledew, 2005). Additionally, accumulation of secreted products to high concentration requires fermentations of >5 days (Phillips et al., 1993; Shen et al., 2014a).

Carbon recycling using GTL biocatalysis utilizes microbes capable of growth on C1 substrates (CO, CH_4, and CO_2). Our model organism is *C. ljungdahlii* OTA1 which converts CO from syngas as its sole carbon source into ethanol and acetate (Koepke et al., 2011; Ragsdale and Pierce, 2008; Tanner et al., 1993). Mutant OTA1 was derived from ATCC 55383 and isolated for its desirable ethanol to acetate ratio and CO consumption (Tirado-Acevedo, 2010; Whitham et al., 2015). Wild-type *C. ljungdahlii* has been shown to have a maximum specific uptake of ~35 mmol CO $g_{DCW}^{-1}\,h^{-1}$ in liquid culture (Mohammadi et al., 2014; Richter et al., 2013).

There have been a number of efforts to reduce power input by reactor design in GTL stirred tank syngas processing by bubble columns, airlift, or immobilized systems such as trickle bed, or microchannel monoliths. Hollow fiber reactors with high surface area for gas processing can operate with cells in suspension (Davis, 2007) or immobilized on the shell side of the fibers (Shen et al., 2014a). As the solubility of CO is fixed by fermentation conditions, most studies focus on improving the carbon monoxide mass transfer coefficient, k_La, as described (equation 1).

$$\mathrm{COTR} = \frac{dn_{\mathrm{CO},l}}{V_{\mathrm{L}}dt} = k_La\left(C^*_{\mathrm{CO},l} - C_{\mathrm{CO},l}\right) \quad (1)$$

were COTR, $n_{CO,l}$, k_La, C^*, C_L, and V_L are the CO transfer rate ($mol\,L^{-1}\ h^{-1}$), moles of CO in the liquid phase, overall mass transfer coefficient (h^{-1}), the maximum CO solubility ($mol\,L^{-1}$), the concentration of CO in the liquid phase ($mol\,L^{-1}$), and the liquid volume, respectively.

Both suspension and immobilized whole cell systems can be mass transfer limited. In order to achieve high production rates and product titers, suspension systems need cell recycle to retain the catalyst. However, at very high cell density, mass transfer of nutrients as well as gaseous substrate may limit the productivity per g_{DCW} (Richter et al., 2013). Many immobilized cell and trickle bed systems demonstrate elevated mass transfer but rely on the organism's ability to form a uniform thin biofilm with good adhesion and the volume of gas in the reactor is low due to the volume of the inert packing material (Shuler, 2002).

What is needed to continuously process large volumes of low solubility gaseous carbon is to significantly reduced power for gas-liquid mass transfer, intensify volumetric gas uptake rates, enhance microbial specific productivity, decrease reactor size, stabilize biocatalyst half-life, minimize water/medium required, and increase product concentration for more efficient purification. One approach is to apply the concepts of process intensification (PI) from chemical reactor technology to bioprocessing to reduce footprint and increase volumetric reactivity (Hessel et al., 2013; Jenck et al., 2004; Kumar and Nigam, 2012; Vaccaro et al., 2014; Wiles and Watts, 2012). Previous work on bioprocess intensification has been focused on colonization of macroporous monolith supports with the limitations of reactor channeling, non-uniform flow and large pressure drops in a gas/liquid system (Akay et al., 2005).

In order to address mass transfer and reactivity limitations and to increase the volume of gas in the reactor, we propose a proof-of-concept thin film bioreactor. The reactor will not use suspended cells but a biocomposite material: cells immobilized at very high concentration on paper, an inexpensive wetted flexible nonwoven porous matrix. Cells in a non-growth state can be adsorbed onto cellulose fibers in a nonwoven paper support with controlled loading (coating) for uniform reactivity. This approach concentrates their syngas absorbing reactivity over a defined nominal surface area with the gas phase separated from the microbes by a thin liquid film (Gosse et al., 2012). The gas phase now dominates the reactor (high gas fraction). This approach will enable designing falling film continuous bioreactors where the liquid phase flows down the biocomposite (on the surface and through the paper pores space) as a very thin film generated at low Reynolds number with co- or counter-current gas flow. As mass transfer and film thickness are inversely related, elevated mass transfer at low power input can be achieved. Falling film chemical reactors demonstrate very high mass transfer rates in, for example, nitrobenzene hydrogenation (~10,000 h^{-1}). Because of the small liquid phase volume, the interfacial area, a, can be as high as 20,000 $m^2\,m^{-3}$ of reactor volume or higher in contrast to bubble columns and agitated tanks which rarely exceed interfacial areas of 200 $m^2\ m^{-3}$ (Hessel et al., 2005).

Biocomposite materials may address the limitations of batch GTL C1 carbon recycling and the observed slow specific rates of *C. ljungdahlii* as well as other C1 utilizing organisms when used in suspend bioreactors. By limiting nutrients so the biocomposite-entrapped cells are non-growing but metabolically active, the biocatalyst can operate at a constant rate without deactivation or generating waste biomass. Preliminary studies by our group on small surface area paper biocomposites in vertical tubes demonstrated sustained reactivity for over 300 h for *C. ljungdahlii* OTA1 and 100 s of hours for photosynthetic microorganisms (Bernal et al., 2014; Gosse et al., 2012). A submerged H_2 generating photoreactive biocomposite coating of *Rhodopseudomonas palustris* on polyester strips demonstrated continuous reactivity at a constant rate without cell outgrowth for over >4000 h when periodically supplied with acetate (Gosse et al., 2010). Using biocomposites was shown to intensify specific consumption rate by ~5 to 10-fold for gas absorbing *Synechococcus* (Bernal et al., 2014) and increase the effectiveness factor of a *Gluconobacter* biotransformation by 20-fold (Fidaleo et al., 2006).

Here we report advances over our previous syngas biocomposite work (Gosse et al., 2012) by using slowly shaking horizontal tubes with increased coating surface area and reduced liquid volume. This new configuration demonstrates increased specific CO consumption, enhanced specific product production rate and permits estimation of power requirements.

Materials and Methods

Computational Methods

A simplifying assumption for solving for k_La is assuming $C_{CO,l} \approx 0$. This is reasonable if there is a high concentration of active

C. ljungdahlii OTA1. This assumption provides a minimal estimate for k_La referred to as the apparent overall mass transfer coefficient, $k_La_{app.}$ Rearranging equation 1 yields:

$$k_{\mathrm{L}}a_{\mathrm{app}} = \frac{\mathrm{COTR}}{C^*_{\mathrm{CO,l}}} \tag{2}$$

Estimation of the solubility of CO in the liquid phase was done using the initial partial pressure of CO and the Henry's constant corrected for temperature (Sander, 2015). In a batch system, C^* will change as a function of time; this assumption gives a minimal estimate of k_La.

Methods for estimating the power consumption of a shaking vessel is challenging but have been described (Buchs et al., 2000a,b; Kato et al., 1995). Modifications to the method of Buchs et al. (2000b) were employed for horizontal tubes to estimate shaking power requirements using the Reynolds (*Re*) number:

$$Re = \frac{\rho n d^2}{\eta} \tag{3}$$

where ρ, n, d, and η are the liquid density, shaking frequency, maximum inner shaken flask diameter, and dynamic viscosity, respectively. *Re* was empirically correlated with a modified power number Ne′ by:

$$Ne' = \frac{P}{\rho n^3 d^4 V_{\mathrm{L}}^{1/3}} = 70Re^{-1} + 25Re^{-0.6} + 1.5Re^{-0.2} \tag{4}$$

where V_L is the liquid volume in the shaking system. Equation 4 can be rearranged to solve for power consumption:

$$\frac{P}{V} = Ne'\rho\frac{n^3 d^4}{V_{\frac{2}{3}}^{\frac{2}{3}}} \tag{5}$$

P and V are the power requirement and liquid volume, respectively. Solving equation 5 gives an estimate of the power requirements at different shaking frequencies for liquids agitated by shaking in horizontal tubes where *Re* is low. The interior surface area of a horizontal tube that a known liquid volume covers at rest was calculated as d defined as a circle of the same area. Buchs cautions that when Re is less than 10^4, the shaking may lead to the liquid being "out-of-phase" where portions of bulk liquid are motionless. That may lead to errors in the estimated power consumption (equation 4). This type of motion may be occurring in slowly shaking horizontal tubes especially at the very low liquid volume and shaking frequencies where Re $\sim 10^3$. However, those errors are always an overestimation of the power requirement (Buchs et al., 2000b).

Bacterial Strain, Media, and Growth Conditions

C. ljungdahlii OTA1, a mutant of *C. ljungdahlii* that has shown oxygen tolerance and improved product ratio (provided by Dr. Amy Grunden, NCSU) (Tirado-Acevedo, 2010) was used as a model syngas absorbing organism. The growth medium, modified clostridial medium with fructose (mRCMf), was prepared as previously described (Cotter et al., 2009) excepting that the pH was adjusted to 6.3. Each 160 mL serum bottle received 93 mL of medium and the headspace was 45% CO/45% H_2/10% N_2. In order to limit outgrowth from the biocomposite, 1YCM, was prepared as previously described (Gosse et al., 2012) with 5 g L^{-1} 4-morpholineethanesulfonic acid (MES hydrate SIGMA, St. Louis, MO) added and the pH was adjusted to 6.0 with 5 M KOH. Each 160 mL serum bottle received 50 mL of medium and flushed with the gas mixture above. The reducing agent solution was prepared in an anaerobic chamber by mixing 2.5 g cysteine HCl with 100 mL of anoxic water in a 160 mL serum bottle. The bottle was stoppered in the anaerobic chamber (Chemglass, Inc., Vineland, NJ), the stopper crimped and flushed for 5 min at 5 psig with argon then pressurized to 20 psig. The bottle was autoclaved for 20 min and stored in the dark at room temperature. At least 12 h before use, 1YCM and mRCMf were reduced aseptically with 1 and 2 mL per serum bottle, respectively, of reducing solution.

Preparation of Coating Suspension

A mid-log cell suspension ($OD_{600} = \sim 1.3$) was transferred to two autoclaved 50 mL Oak Ridge centrifuge tubes sealed with silicone gasket caps in an anaerobic chamber. The cells were centrifuged at 4°C for 15 min at 6,000 *g* and then the tubes moved into the anaerobic chamber. The supernatant was decanted, the pellet rinsed by resuspending in 1YCM, and then centrifuged at 4°C for 15 min at 6,000 *g*. After decanting the supernatant, the pellet was mixed by vortexing until homogenous. Coating emulsion was prepared by adding cell paste to 1YCM at 30% (v/v) and applied at 6.5 g DCW/m^2. Cell loadings were estimated using 363 mg dry cell weight OTA1 L^{-1} OD_{600}^{-1} and 1.9E8 CFU OTA1 mL^{-1} OD_{600}^{-1} (data not shown).

Coating of Paper Substrate

3MM chromatography paper (Whatman) was prepared by cutting into strips (2×10 or 2×5 cm, 335 μm thick), wrapped in aluminum foil, autoclaved for 20 min (dry cycle), and stored in the anaerobic chamber. The coating solution was applied by pipette extrusion by evenly distributing 100 μL of coating suspension per 5 cm^2 of paper surface area in the anaerobic chamber (5%H_2/ balance Ar, 25°C, 48% relative humidity). Only half the paper strip was coated so that the coated portion would remain above the liquid level when the tube was horizontal.

Preparation of Batch Tube Gas Absorber/Reactors

Coated papers were immediately placed into autoclaved Balch tubes (~26 mL working volume) and hydrated. For suspended cell studies, the same volume of coating solution was added directly to the tube (without a paper support) and additional medium was added. Tubes were stoppered (Geo-Microbial Technologies, Inc., Ochelata, OK) in the anaerobic chamber, removed from the chamber, capped and crimped with aluminum seals. The tubes were then flushed with syngas mixture for 2 min

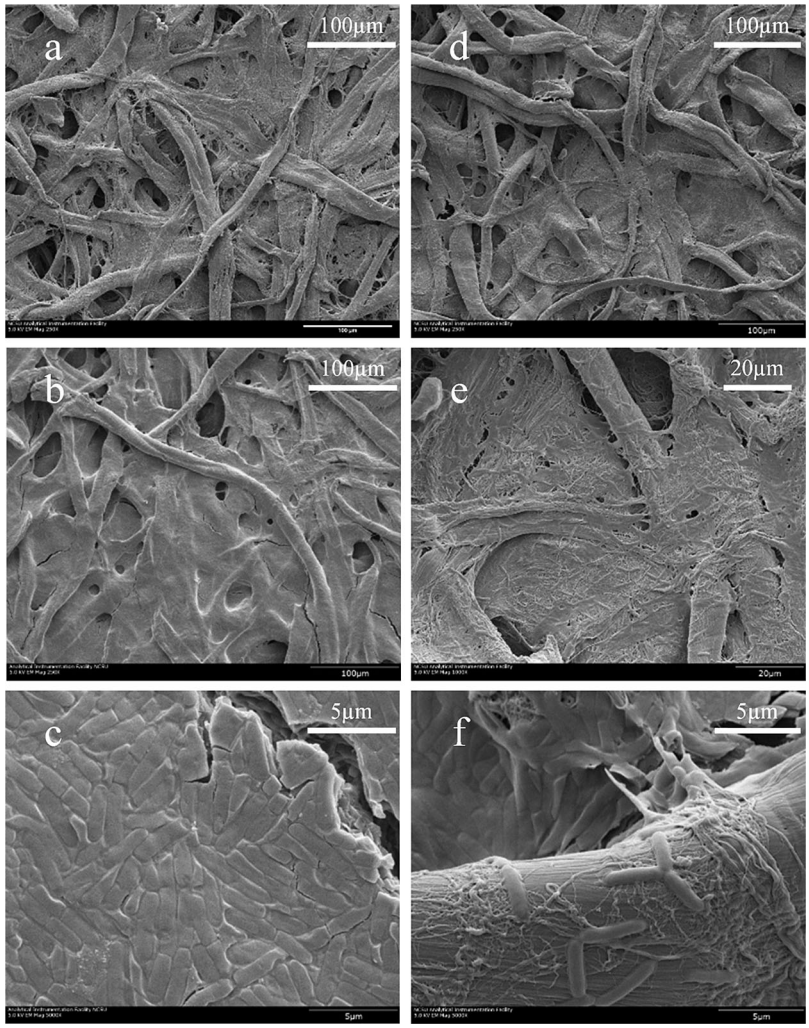

Figure 1. SEM images of 3MM paper substrates and biocomposite coatings showing concentrated cell patches and cells adsorbed on top of cellulose fibers. (**a**) Bare Whatman 3MM chromatography paper (**b**) Coating of ~11 g m^{-2} (**c**) High magnification image of ~11 g m^{-2} multilayered cell coating (**d**) Cell loading of ~4.4 g/m^2 (**e, f**) High magnification images of ~4.4 g m^{-2} cell coating.

at 5 psig, and then vented to atmospheric pressure. The tubes were then placed horizontally with tape holding the tubes so that the paper substrate remained vertically oriented in a shaker (Infors-HT, Multitron Standard, Laurel, MD) with a 25 mm diameter of rotation at 37°C. A single gas sample was taken from each tube to calculate the consumption rate. Care was taken to ensure data was taken before 2/3 of the CO was consumed (normally after 3–5 h) as further incubation demonstrated that the reactivity deviated from linearity due to decreased syngas driving force. Production data was obtained by making 30 tubes. At each time point three from each condition were sampled for gas, then sacrificed to withdraw the liquid sample.

Determination of the cell adsorption capacity and optimal coating concentration of the 3MM cellulose fibers was by rinsing freshly prepared biocomposites and putting the paper strips upright into horizontal anaerobic tubes on the shaker at 100 rpm and 37°C. After 3.5 h of shaking the tubes were placed into the anaerobic chamber, the biocomposites moved to new tubes with fresh medium, and the tubes containing the original medium resealed. All of the tubes were then capped, crimped, flushed, and placed in the shaker for 17 h before assaying gas consumption.

Gas Analysis

Headspace gas analysis (H_2, O_2, N_2, CO, and CO_2) was performed using an Agilent 7890 gas chromatograph containing a Supelco 60/80 mole sieve 5A column (6' × 1/8" × 2.1 mm SS) and a thermal conductivity detector. The GC was fitted with a custom sample tube to allow direct injection of the 1 mL gas sample from the gas tight syringe (SGE Analytical Science, Austin, TX) into the 10 µL sample loop. Argon was the carrier gas at 20 mL/min for 1.5 min then increased to 32 mL/min and held for 3.4 min. Oven temperature was held at 170°C for 1.5 min then a ramp of 75°C/min to 240°C and

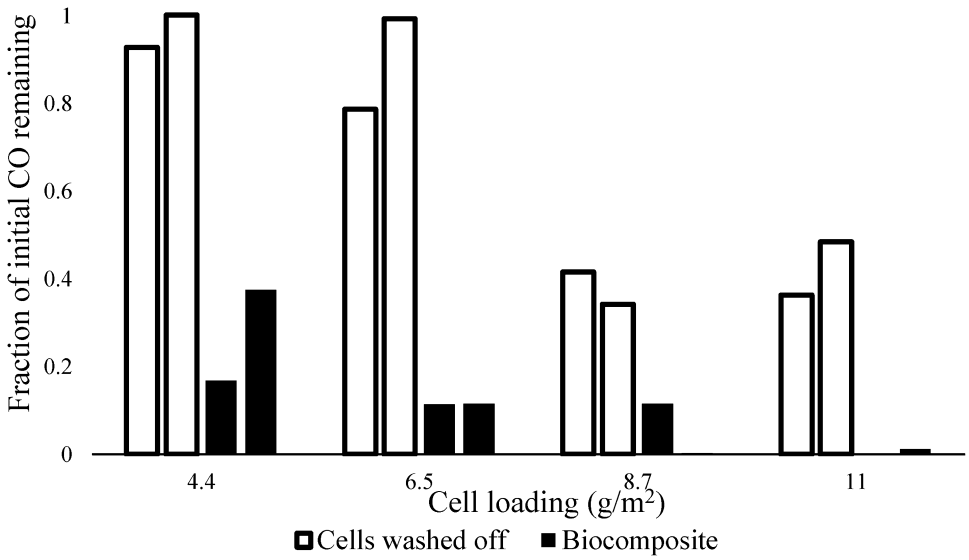

Figure 2. Comparison of reactivity of *C. ljungdahlii* OTA1 rinsed off of a biocomposite as a function of different cell loadings by adsorption. Cells removed from biocomposite by shaking at 100 rpm with transfer to a new tube with gas flushing. Both duplicates shown.

held for 3.4 min. Total run time was 5.9 min. Injector and detector temperatures were 160 and 250°C, respectively. Peak areas were scaled relative to the unconsumed nitrogen peak and converted to moles consumed per hour.

Liquid Analysis for Ethanol and Acetate

Liquid samples (~1 mL) were removed from anaerobic tubes and frozen in microcentrifuge tubes at −20°C. When assayed, the

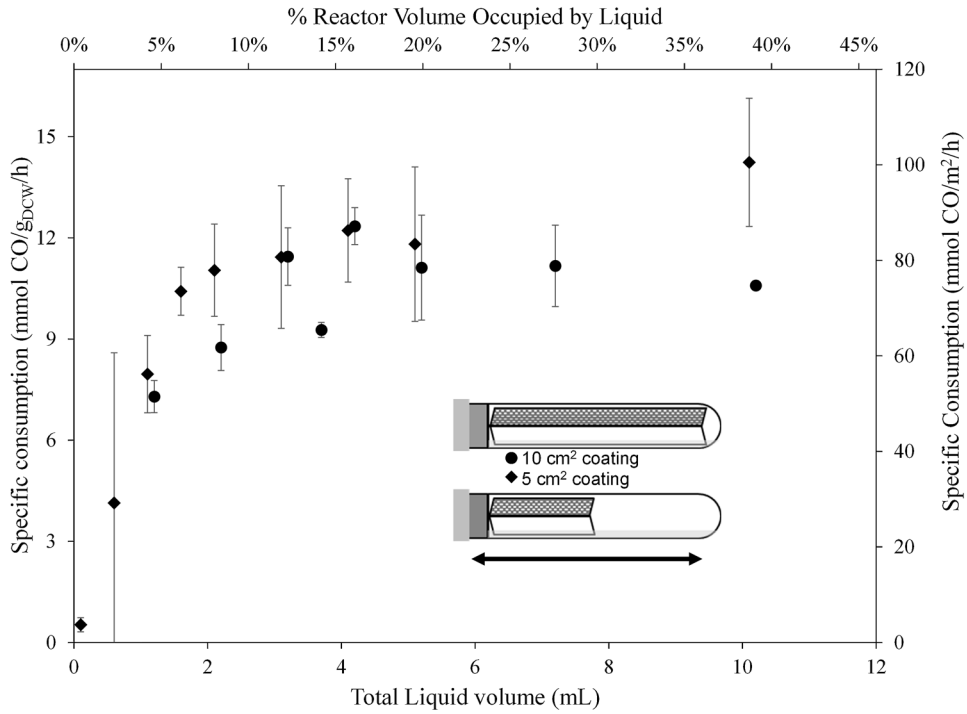

Figure 3. Comparison of CO uptake reactivity in horizontal Balch tubes with different liquid medium volume. Each data point can be read from either axis: per gram dry cell weight or per m^2 of coating area. Reactivity stays elevated until liquid medium volume is ~ <4 mL or ~15% of reactor volume. Triplicate determinations, $n = 3$. 20 cm^2 3MM paper substrate with a 10 cm^2 coated area shown. Liquid phase is depicted on the bottom of the horizontal tubes. Shaking agitation depicted by arrow.

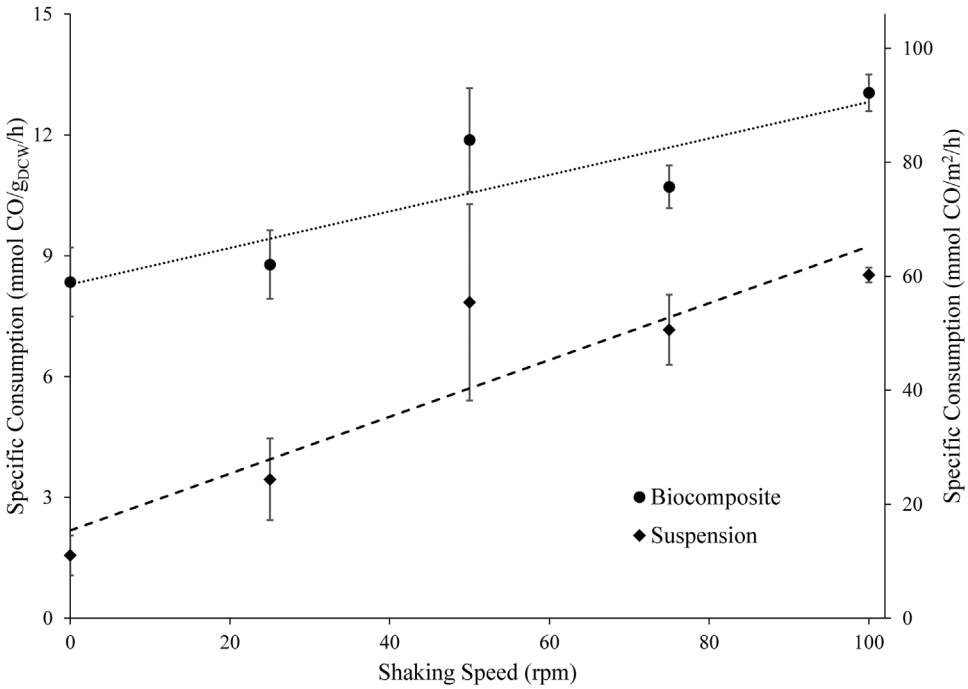

Figure 4. Comparison of CO reactivity versus shaking speed for a biocomposite and the same number of cells in suspension in 4 mL of medium in horizontal tubes. Data can be read from either axis. Triplicate determinations.

micro-centrifuge tubes were thawed and centrifuged at 13,000 rpm for 5 min and 150 μL of the supernatant was added to 37.5 μL of 2.5% (m/v) m-phosphoric acid in a fresh tube. The samples were then mixed by vortexing and 120 μL was added to 2 mL amber vial with septum tops (Fisherbrand) with target micro-serts (National Scientific). The vials were analyzed with an Agilent 7890A gas chromatograph using a J&W scientific PEG acid modified column 30 m × 0.25 mm ID with a 0.5 μm film (DB-FFAP 122-3233), a flame ionization detector, and an autoloader. Oven temperature was held at 75°C for 1 min then a ramp of 25°C/min to 200°C and held for 5 min. The inlet and detector temperatures were both 250°C. The hydrogen flow rate was 40 mL/min and air was 400 mL/min. The injection was 0.5 μL with at 10:1 split ratio sent to the column with argon as the carrier gas.

Samples evaluated for enhanced product recovery from the biocomposite were upended 25 times over 1 min ensuring the liquid passed over the coated portion of the biocomposite. Before beginning enhanced recovery, the medium was clear. After rocking, the cells came off into the medium making it turbid.

Biocomposite Characterization

Images of *C. ljungdahlii OTA1* biocomposites were taken at the Analytical Instrumentation Facility (AIF) at NC State University using methods described previously (Bernal et al., 2014).

Static film thickness was estimate by a vertically oriented micrometer (Mitutoyo Absolute) with one end of the 3MM chromatography paper sitting in tap water for increased conductivity. An ohmmeter was attached to the manually advanced plunger of the micrometer and the wetted biocomposite. Thickness measurements were recorded when the ohmmeter values changed dramatically.

Results and Discussion

SEM images of the microstructure of *C. ljungdahlii* paper coatings are shown in Figure 1. Initial coatings of 11 g m^{-2} nominal surface area showed a loss of macroporosity. Decreasing the loading to 4.4 g m^{-2} reduced blocking of the paper pores. In this study, no adhesive latex polymer binders were used to bind the cells to the 3MM paper in contrast to previous work (Bernal et al., 2014; Gosse et al., 2012).

We investigated cell adhesion to the 3MM paper by measuring retention of CO absorbing activity. We compared consumption data on the biocomposite in a fresh tube and the cells washed off into the rinse medium (Fig. 2). At the higher cell loadings (8.7 and 11 g/m^2) significant reactivity remained in the liquid phase after removing the biocomposite. At the lowest two loadings, 4.4 and 6.5 g/m^2, there is minimal reactivity remaining in the liquid phase after the biocomposite is removed. The loading of 6.5 g/m^2 was chosen for further experiments.

Previous *C. ljungdahlii* OTA1 paper biocomposite studies used a latex binder and hydrated the cells immediately after coating with 10 mL of minimal medium in a vertical Balch tube (Gosse et al., 2012). In this study, placing the tubes horizontally enabled a larger coated surface area in contact with the gas phase. Reducing the medium volume did not decrease CO absorption reactivity until ∼4 mL per tube. (Fig. 3). This was unchanged for coating

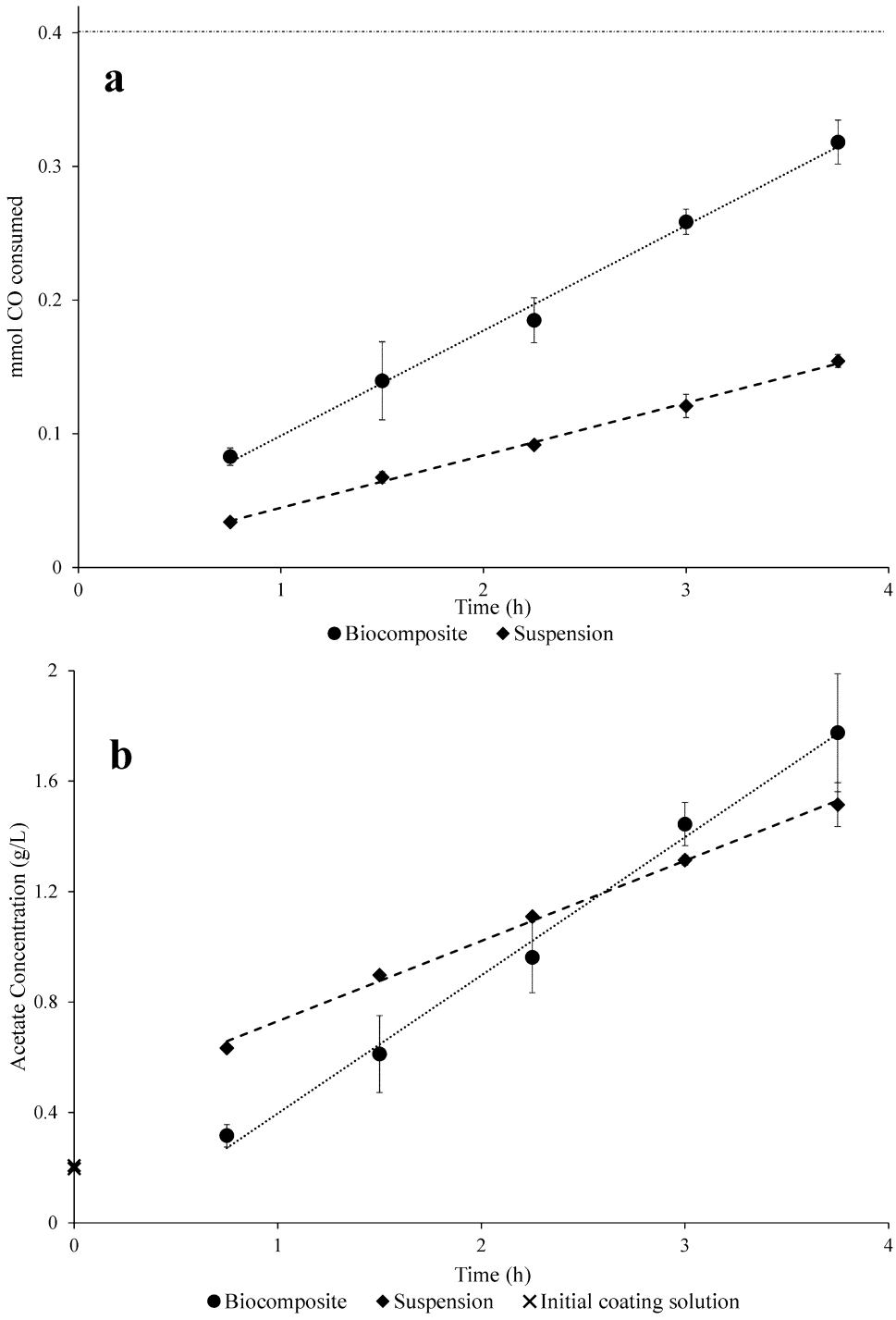

Figure 5. A time course comparing both gas consumption (**a**) and liquid product production (**b**) for biocomposites (circles) and suspended cells (diamonds) at 50 rpm. Triplicate determinations. The dotted line along the top of (a) show the total initial CO present. Both replicates of the initial coating solution are shown as crosses.

surface area of 5 or 10 cm^2; the reproducibility of our data for both configurations was high. Using 4 mL of medium per tube decreased liquid volume by 60% on a reactor volume basis, and 69% and 85% on a coating surface basis for the 5 cm^2 and 10 cm^2 biocomposite. The medium volume was decreased to 15% of total reactor volume while the CO consumption per m^2 of paper was intensified by ~14-fold over previous work (Gosse et al., 2012) 6.6 versus ~90 mmol CO m^{-2} h^{-1}.

A comparison of the liquid volumes (4, 6, 8 mL) after the biocomposite had consumed 100% of the CO showed the greatest increase in secreted product concentrations at the lowest liquid volume. Normalizing the data to the amount of gas initially present

Table I. CO consumption and mass transfer parameters (26 mL reactor volume, 4 mL medium).

Condition	Cell mass (mg)	Nominal coating surface area (cm^2)	CO Consumption Rate ± SE ($n = 3$)				
			mmol m^{-2} h^{-1}	mmol$g_{DCW}^{-1}h^{-1}$	mmol$L_{Liquid}^{-1}h^{-1}$	mmol$L_{Reactor}^{-1}h^{-1}$	$k_La_{apparent}$ (h^{-1})
Suspended	6.5	N/A	N/A	4.6 ± 0.085	10 ± 0.2	1.5 ± 0.03	26
Biocomposite	3.3	5	90 ± 13	14 ± 2.0	11 ± 1.6	1.7 ± 0.24	30
	6.5	10	87 ± 2.0	13 ± 0.31	22 ± 0.5	3.3 ± 0.08	56
	13	20	94 ± 2.4	14 ± 0.37	47 ± 1.2	7.2 ± 0.18	116

and subtracting the argon headspace control showed that 4 and 6 mL liquid volumes had 80% and 26%, respectively, higher total acetate concentration than 8 mL. This increase in product concentration is without engineering the cell. The final secreted products in the 4 mL tube were 4.3 ± 0.21 g/L with a 0.052 ± 0.0054 ethanol/acetate ratio (triplicate determinations, mol/mol). This is a ~150% yield from the initial amount of CO which is the only carbon source provided in the medium 1YCM. That indicates some unfermented fructose remained surrounding or inside the cells through the rinse step. However, it is the same for all cases investigated. The ethanol/acetate ratio is much lower than reported elsewhere in the literature for research focusing on optimizing ethanol production (Gaddy et al., 2007; Yasin et al., 2015).

A comparison of the specific reactivity of OTA1 in suspension in the horizontal tubes showed that the biocomposite outperformed the suspended cells at all the shaking speeds <100 rpm (Fig. 4). At 0 rpm, the biocomposite outperforms cells in suspension by >5-fold. Using equations 3–4, the estimated power requirements of the different shaking conditions (except 0 rpm) were compared. At 25, 50, 75, and 100 rpm the power requirements are 0.21, 1.2, 3.6, 7.7 $W m^{-3}$, respectively. Comparing the biocomposite at 100 versus 25 rpm, a reduction of the power requirement by 97% reduced the CO consumption rate by only 36%.

Both the biocomposite and suspended cells have reactivity that is dependent upon power input (shaking speed). The biocomposite reactivity is dependent upon shaking speed likely because of the increased flow of medium into and out of the paper pores providing the cells with nutrients and removing secreted products. Figure 4 shows that the suspended cells are >50% more dependent on the power input (steeper fit) while having a lower reactivity. A least squares fit of this data predicts a crossover at ~250 rpm where suspended cells will outperform a biocomposite. The power requirement at 250 rpm is 89 $W m^{-3}$, >11-fold higher than at 100 rpm, and >420-fold higher than at 25 rpm.

A time course experiment was performed to compare gas consumption and product production at 50 rpm. The CO consumption results (Fig. 5a) show the biocomposite outperforming the same number of suspended cells by >2-fold. In contrast to the lag in reactivity due to formation of a biofilm, the reactivity of the biocomposite is detected immediately. The liquid product production results are not as dramatic (Fig. 5b). Only acetate production is shown due to a negligible amount of ethanol produced (<0.1 $g L^{-1}$). Before ~2.5 h, more acetate is found in the liquid phase of the suspended cells. After that point, there is more acetate in the liquid phase of the biocomposite tubes, but less than predicted. The liquid products may be concentrated in the pores of the paper substrate as there is no forced fluid flow in the pore space of this batch system. In a flowing thin film system the rate of products flowing out of the biocomposite pores will be increased. The simple shaking tube system demonstrates a biocomposite final acetate titer of 1.8 $g L^{-1}$ and an acetate production rate of ~0.5 $g L^{-1} h^{-1}$.

Table I shows that the specific CO consumption rate per area almost constant across the three biocomposite conditions evaluated. The 5 cm^2 biocomposite has almost identical

Table II. Production characteristics and reactor comparison.

Reactor type	Notes	Ethanol: Acetate (mol/mol)	C_2 production rate ± SE ($n = 3$)		Ref
			mmol$L_{Liquid}^{-1}h^{-1}$	mmol m^{-2} h^{-1}	
Suspended cells	Batch	0.001	8.2 ± 0.04	N/A	This work
Biocomposite	10 cm^2 batch	0.001	7.8 ± 0.4	31 ± 1.6	This work
	10 cm^2 batch enhanced recovery	0.001	10 ± 0.5	40 ± 2.1	This work
	5 cm^2 batch enhanced recovery	0.003	5.4 ± 1.0	43 ± 7.8	This work
	20 cm^2 batch enhanced recovery	0.002	23 ± 0.6	46 ± 1.3	This work
STR	Continuous cell recycle	21	1.95	N/A	Phillips et al. (1993)
STR	Continuous cell recycle	2.2	2.22	N/A	Liu et al. (2014)
STR	Continuous gas batch liquid 100 L pilot	5.2	0.79	N/A	Kundiyana et al. (2010)
STR	High pressure optimized media cell recycle continuous	12	240	N/A	Gaddy et al. (2007)
Bubble	Cell recycle continuous	3.0	9.7	N/A	Richter et al. (2013)
Monolith	Cell recycle continuous gas batch liquid	2.1	3.2	6.6	Shen et al. (2014b)
HFMR	Cell recycle continuous gas batch liquid	1.5	5.1	29	Shen et al. (2014a)
HFMR	Continuous cells embedded in membrane	3.3	5.4	51	(Tsai et al. (2012)

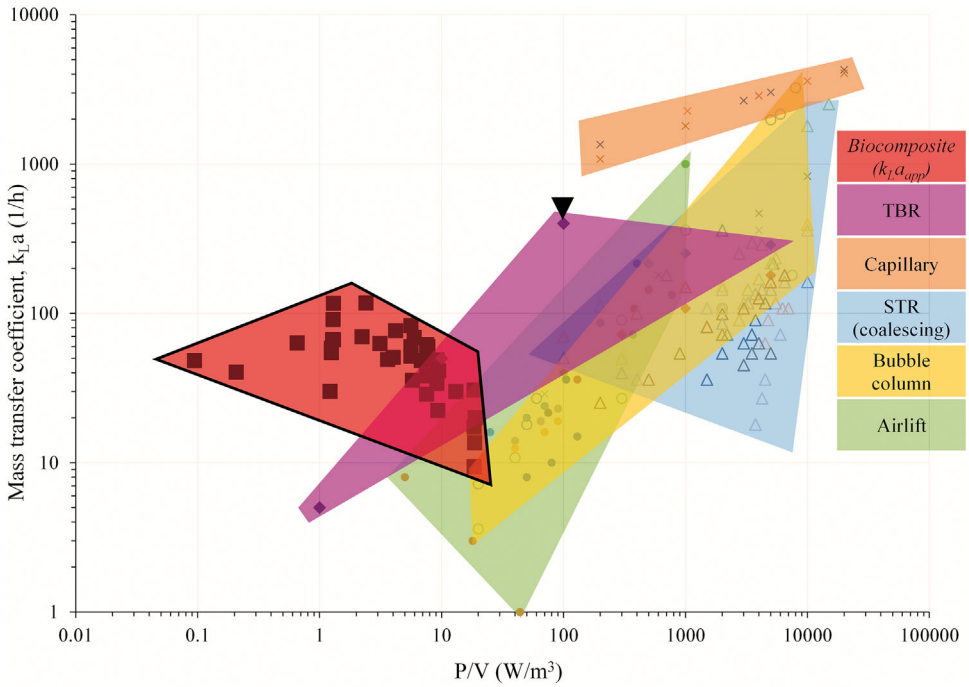

Figure 6. Comparison of mass transfer coefficient with power input. Symbols are: open triangle-stirred tank (Arjunwadkar et al., 1998; Boodhoo et al., 2008; Bredwell et al., 1999; Garcia-Ochoa and Gomez, 2009), open circle-bubble column (Linek et al., 2005), closed diamond-trickle bed reactor (Bredwell et al., 1999; Kraakman et al., 2011), closed circle-airlift reactor (Bredwell et al., 1999; Gourich et al., 2006; Loubiere et al., 2009; Pirouzi et al., 2014), cross hatch-monolith or microchannel (Kraakman et al., 2011; Kreutzer et al., 2005), black squares-3MM paper biocomposites. Inverted filled triangle is test case to confirm power calculations. All data is presented in terms of a mass transfer coefficient for O_2.

performance to the suspended cells even though this biocomposite has half the number of cells. The reactivity per volume of liquid or total reactor volume increases linearly with coated surface area. Because increasing biocomposite surface area with constant liquid volume increases interfacial area, *a*, the apparent mass transfer coefficient, k_La_{app}, increases linearly without additional power for mass transfer.

Table II compares the liquid product production results with literature data. Although the biocomposite absorbed ~2-fold more CO, it produces the same amount of secreted products. With

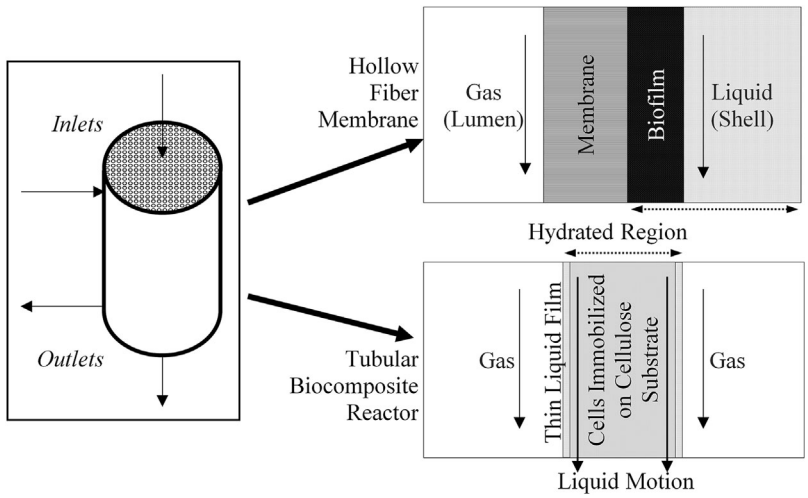

Figure 7. Comparison between a hollow fiber and biocomposite reactor. In hollow fiber reactors the membrane separates the gas and liquid phase with the biofilm forming in the shell or bulk liquid phase. The biocomposite has concentrated cells embedded within the tube walls with gas on both sides with the liquid moving through the paper pores and over the surface of the biocomposite in a thin liquid film that minimizes mass transfer resistance.

enhanced recovery (mixing) to mimic a falling film (to enhance flow of secreted products out of the paper pores), the biocomposite outperforms the same number of suspended cells by only 22%. More work is needed to optimize the cellulose paper structure (pore space) so that products are not trapped in the paper. Secreted product per volume productivity scales approximately linearly with nominal coating area and productivities per area are approximately the same across all the enhanced recovery samples. The highest nominal surface area biocomposite specific volumetric production rate exceeds almost all the examples in the literature except for a high pressure, optimized media, cell recycle CSTR (Gaddy et al., 2007). The specific production rate per unit area also outperforms the data where the calculation can be made but from Coskata, Inc. (Tsai et al., 2012). The Coskata method involves a membrane with imbedded cells; not unlike a biocomposite.

The data from Figures 3, 4, and Table I were evaluated using equation 2 to obtain a minimal estimate of the mass transfer coefficient, $k_L a_{app,}$ and plotted in relation to their calculated power requirements to compared with other reactor types (Fig. 6). (Arjunwadkar et al., 1998; Boodhoo et al., 2008; Bredwell et al., 1999; Garcia-Ochoa and Gomez, 2009; Gourich et al., 2006; Kraakman et al., 2011; Kreutzer et al., 2005; Linek et al., 2005; Markopoulos et al., 2007; Pirouzi et al., 2014) Experimental results for $k_L a_{app}$ generated experimentally are for CO and converted into mass transfer coefficients for O_2 for proper comparison using a ratio of the square root of the diffusivities (Danckwerts, 1951).

In order to confirm that the biocomposite results are reasonable, it was determined that 264 rpm shaking speed would be $\sim$100 W m^{-3} and the $k_L a_{app}$ was calculated and found to be similar for cells in suspension (inverted triangle, Fig. 6) just above the trickle bed regime which is expected because of the small liquid phase volume being spread into a thin film on the tube's inner surface at this elevated shaking speed.

The biocomposites' minimal estimated $k_L a_{app}$ in this simple system is lower than some of the $k_L a$ values reported for other bioreactors. However, the actual value will be higher. Our data indicates a $k_L a_{app}$ for CO of $\sim$100 h^{-1} with a power requirement that is one to four orders of magnitude lower than reported for other bioreactor types and matches or exceeds mass transfer rates reported for syngas fermentations (Munasinghe and Khanal, 2010; Yasin et al., 2015). The presence of CO consuming microorganisms will increase the observed mass transfer coefficient if mass transfer is limiting (Garcia-Ochoa and Gomez, 2009). By using the nominal reactive paper surface area and measuring film thickness, k_L can be estimated. The static liquid film thickness on top of the paper was measured to be $\sim$130 μm. Assuming a flat film over the cells and no bubbles or wavelets, the interfacial area is $\sim$8000 m^{-1} and k_L is therefore $\sim$2E-6 m s^{-1}. A first approximation for a static film is the membrane equation, $kl/D = 1$ (Cussler, 2009) where l is the membrane thickness or in this case, the film thickness. Using the diffusivity of CO in water, k_L is $\sim$2E-5 m s^{-1} or a full order of magnitude higher than what we observe experimentally. Gas-to-liquid mass transfer is not limiting in this configuration. The system is limited by the cells' metabolism (see also the specific uptake rates in Table I). These small surface area biocomposite rates are below the maximum reported in literature for dilute suspended cells, 14 versus 35 mmol g_{DCW}^{-1} h^{-1}. The suspended cell maximum uptake rate is likely not reached because some cells are entrapped in the interior of the paper using this simple extrusion method and all of the substrate may be consumed by the cells on the surface. Thinner coatings or thinner papers with uniformly coated cellulose fibers should diminish this effect.

A continuous falling film CO absorber system could be constructed of multiple parallel biocomposite tubes mounted inside larger tubes to intensify reactor volumetric reactivity (mmol $L_{Reactor}^{-1}$ h^{-1}) (Fig. 7). This design is conceptually different from hollow fiber bioreactors. In a biocomposite reactor, the cells would be immobilized in nonwoven tubes prior to reactor module construction and there is no bulk liquid phase either inside or outside the tube lumen. A minimal liquid volume moves within the paper pores (within the nonwoven tube walls) while the humidified gas in contact with a thin liquid film will move on the tube surface.

Conclusions

Carbon monoxide consumption as well as acetate production was investigated in a batch system in suspension and using a paper-based biocomposite coated by extrusion without adhesive binders. The biocomposite outperformed the same number of cells in suspension in CO specific uptake rates, specific acetate production rate, and final acetate titer. Methods were presented for estimating the mass transfer coefficient and power required. The biocomposite data compared favorably with stirred tank bioreactors at one to four orders of magnitude less power. Stabilization of *C. ljungdahlii* OTA1 paper biocomposites by engineered adhesion, optimizing paper surface charge, coating microstructure, cellulose fiber coverage and dry stabilization are currently being investigated by our group. The reduced mass transfer power input and CO uptake intensification shown is a proof-of-concept of thin falling film biocomposite reactor approach for GTL processes to recycle gaseous carbon utilizing microbes.

This research was supported by the North Carolina Biotechnology Center (NCBC), the National Institutes of Health Molecular Biotechnology Training Program (T32 GM008776-11), and the Golden LEAF Biotechnology Training and Education Center (BTEC) at NCSU. We acknowledge Dr. Amy Grunden and Dr. Mari Chinn for material support including cultures of *C. ljungdahlii* OTA1 as well as Michael Ray and Kit Yeung for instrumentation support.

References

Abubackar HN, Veiga MC, Kennes C. 2011. Biological conversion of carbon monoxide: Rich syngas or waste gases to bioethanol. Biofuels Bioprod Biorefining 5:93–114.

Akay G, Erhan E, Keskinler B. 2005. Bioprocess intensification in flow-through monolithic microbioreactors with immobilized bacteria. Biotechnol Bioeng 90:180–190.

Arjunwadkar S, Sarvanan K, Kulkarni P, Pandit A. 1998. Gas-liquid mass transfer in dual impeller bioreactor. Biochem Eng J 1:99–106.

Bayrock DP, Ingledew WM. 2005. Ethanol production in multistage continuous, single stage continuous, Lactobacillus-contaminated continuous, and batch fermentations. World J Microbiol Biotechnol 21:83–88.

Bengelsdorf FR, Straub M, Duerre P. 2013. Bacterial synthesis gas (syngas) fermentation. Environ Technol 34:1639–1651.

Bernal OI, Mooney CB, Flickinger MC. 2014. Specific photosynthetic rate enhancement by cyanobacteria coated onto paper enables engineering of highly reactive cellular biocomposite "leaves". Biotechnol Bioeng 111:1993–2008.

Boodhoo KVK, Vicevic A, Cartwright CD, Ndlovu T, Toogood EC. 2008. Intensification of gas-liquid mass transfer using a rotating bed of porous packings for application to an *E. coli* batch fermentation process. Chem Eng J 135:141–150.

Bredwell M, Srivastava P, Worden R. 1999. Reactor design issues for synthesis-gas fermentations. Biotechnol Prog 15:834–844.

Buchholz K. 2012. Biocatalysts and enzyme technology. Weinheim: Wiley-Blackwell.

Buchs J, Maier U, Milbradt C, Zoels B. 2000a. Power consumption in shaking flasks on rotary shaking machines: I. Power consumption measurement in unbaffled flasks at low liquid viscosity. Biotechnol Bioeng 68:589–593.

Buchs J, Maier U, Milbradt C, Zoels B. 2000b. Power consumption in shaking flasks on rotary shaking machines: II. Nondimensional description of specific power consumption and flow regimes in unbaffled flasks at elevated liquid viscosity. Biotechnol Bioeng 68:594–601.

Cotter JL, Chinn MS, Grunden AM. 2009. Ethanol and acetate production by *Clostridium ljungdahlii* and *Clostridium autoethanogenum* using resting cells. Bioproc and Biosys Eng 32:369–380.

Cussler EL. 2009. Diffusion: Mass transfer in fluid systems. Cambridge, NY: Cambridge University Press.

Danckwerts P. 1951. Significance of liquid-film coefficients in gas absorption. Ind Eng Chem 43:1460–1467.

Davis JM. 2007. Animal cell biotechnology: Methods and protocols. In: Pörtner R, editor. Hollow fiber cell culture. Totowa, NJ: Humana Press. p 337–352.

Drzyzga O, Revelles O, Durante-Rodriguez G, Diaz E, Garcia JL, Prieto A. 2015. New challenges for syngas fermentation: Towards production of biopolymers. J Chem Technol Biotechnol 90:1735–1751.

Fidaleo M, Charaniya S, Solheid C, Diel U, Laudon M, Ge H, Scriven LE, Flickinger MC. 2006. A model system for increasing the intensity of whole-cell biocatalysis: Investigation of the rate of oxidation of D-sorbitol to L-sorbose by thin bi-layer latex coatings of non-growing *Gluconobacter oxydans*. Biotechnol Bioeng 95:446–458.

Gaddy JL, Arora DK, Ko C, Phillips JR, Basu R, Wikstrom CV, Clausen EC. 2007. Methods for increasing the production of ethanol from microbial fermentation. USA Patent US7285402.

Garcia-Ochoa F, Gomez E. 2009. Bioreactor scale-up and oxygen transfer rate in microbial processes: An overview. Biotechnol Adv 27:153–176.

Gosse JL, Chinn MS, Grunden AM, Bernal OI, Jenkins JS, Yeager C, Kosourov S, Seibert M, Flickinger MC. 2012. A versatile method for preparation of hydrated microbial-latex biocatalytic coatings for gas absorption and gas evolution. J Ind Microbiol Biotechnol 39:1269–1278.

Gosse JL, Engel BJ, Hui JC-, Harwood CS, Flickinger MC. 2010. Progress toward a biomimetic leaf: 4,000 h of hydrogen production by coating-stabilized nongrowing photosynthetic *Rhodopseudomonas palustris*. Biotechnol Prog 26:907–918.

Gourich B, El Azher N, Vial C, Soulami MB, Ziyad M. 2006. Study of hydrodynamics, mixing and gas-liquid mass transfer in a split-rectangular airlift reactor. Can J Chem Eng 84:539–547.

Hessel V, Angeli P, Gavriilidis A, Lowe H. 2005. Gas-liquid and gas-liquid-solid microstructured reactors: Contacting principles and applications. Ind Eng Chem Res 44:9750–9769.

Hessel V, Kralisch D, Kockmann N, Noel T, Wang Q. 2013. Novel process windows for enabling, accelerating, and uplifting flow chemistry. Chemsuschem 6:746–789.

Jenck J, Agterberg F, Droescher M. 2004. Products and processes for a sustainable chemical industry: A review of achievements and prospects. Green Chem 6:544–556.

Kato Y, Hiraoka S, Tada Y, Shirai S, Ue T, Koh S, Yamaguchi T. 1995. Power-consumption of horizontally shaking vessel with circulating motion. Kagaku Kogaku Ronbunshu 21:365–371.

Koepke M, Mihalcea C, Bromley JC, Simpson SD. 2011. Fermentative production of ethanol from carbon monoxide. Curr Opin Biotechnol 22:320–325.

Kraakman NJR, Rocha-Rios J, van Loosdrecht MCM. 2011. Review of mass transfer aspects for biological gas treatment. Appl Microbiol Biotechnol 91:873–886.

Kreutzer M, Kapteijn F, Moulijn J. 2005. Monoliths as biocatalytic reactors: Smart gas-liquid contacting for process intensification. Ind Eng Chem Res 44:9646–9652.

Kumar V, Nigam KDP. 2012. Process intensification in green synthesis. Green Processing and Synthesis 1:79–107.

Kundiyana DK, Huhnke RL, Wilkins MR. 2010. Syngas fermentation in a 100-L pilot scale fermentor: Design and process considerations. J Biosci Bioeng 109:492–498.

Linek V, Kordac M, Moucha T. 2005. Mechanism of mass transfer from bubbles in dispersions — Part II: Mass transfer coefficients in stirred gas-liquid reactor and bubble column. Chem Eng Process 44:121–130.

Liu K, Atiyeh HK, Stevenson BS, Tanner RS, Wilkins MR, Huhnke RL. 2014. Continuous syngas fermentation for the production of ethanol, n-propanol and n-butanol. Bioresour Technol 151:69–77.

Loubiere K, Olivo E, Bougaran G, Pruvost J, Robert R, Legrand J. 2009. A new photobioreactor for continuous microalgal production in hatcheries based on external-loop airlift and swirling flow. Biotechnol Bioeng 102:132–147.

Markopoulos J, Christofi C, Katsinaris I. 2007. Mass transfer coefficients in mechanically agitated gas-liquid contactors. Chem Eng Technol 30:829–834.

Mohammadi M, Mohamed AR, Najafpour GD, Younesi H, Uzir MH. 2014. Kinetic studies on fermentative production of biofuel from synthesis gas using *Clostridium ljungdahlii*. Sci World J 2014:910590.

Munasinghe PC, Khanal SK. 2010. Syngas fermentation to biofuel: Evaluation of carbon monoxide mass transfer coefficient (k_La) in different reactor configurations. Biotechnol Prog 26:1616–1621.

Phillips JR, Klasson KT, Clausen EC, Gaddy JL. 1993. Biological production of ethanol from coal synthesis gas — medium development studies. Appl Biochem Biotechnol 39:559–571.

Pirouzi A, Nosrati M, Shojaosadati SA, Shakhesi S. 2014. Improvement of mixing time, mass transfer, and power consumption in an external loop airlift photobioreactor for microalgae cultures. Biochem Eng J 87:25–32.

Ragsdale SW, Pierce E. 2008. Acetogenesis and the Wood-Ljungdahl pathway of CO_2 fixation. Biochim Biophys Acta 1784:1873–1898.

Richter H, Martin ME, Angenent LT. 2013. A two-stage continuous fermentation system for conversion of syngas into ethanol. Energies 6:3987–4000.

Sander R. 2015. Compilation of Henry's law constants (version 4.0) for water as solvent. Atmos Chem Phy 15:4399–4981.

Shen Y, Brown R, Wen Z. 2014a. Syngas fermentation of Clostridium carboxidivoran P7 in a hollow fiber membrane biofilm reactor: Evaluating the mass transfer coefficient and ethanol production performance. Biochem Eng J 85:21–29.

Shen Y, Brown R, Wen Z. 2014b. Enhancing mass transfer and ethanol production in syngas fermentation of Clostridium carboxidivorans P7 through a monolithic biofilm reactor. Appl Energy 136:68–76.

Shuler ML. 2002. Bioprocess engineering: Basic concepts. Upper Saddle River, NJ: Prentice Hall.

Tanner R, Miller L, Yang D. 1993. *Clostridium ljungdahlii* sp. nov., an acetogenic species in clostridial rRNA homology group I. Int J Syst Bacteriol 43:232–236.

Tirado-Acevedo O. 2010. Production of bioethanol from synthesis gas using *Clostridium ljungdahlii* as a microbial catalyst (PhD dissertation), North Carolina State University.

Tsai SP, Datta R, Basu R, Yoon SH. 2012. Syngas conversion system using asymmetric membrane and anaerobic microorganism. USA Patent US8329456.

Vaccaro L, Lanari D, Marrocchi A, Strappaveccia G. 2014. Flow approaches towards sustainability. Green Chem 16:3680–3704.

Whitham JM, Tirado-Acevedo O, Chinn MS, Pawlak JJ, Grunden AM. 2015. Metabolic response of *Clostridium ljungdahlii* to oxygen exposure. Appl Environ Microbiol 81(24):8379–8391.

Wiles C, Watts P. 2012. Continuous flow reactors: A perspective. Green Chem 14:38–54.

Wilkins MR, Atiyeh HK. 2011. Microbial production of ethanol from carbon monoxide. Curr Opin Biotechnol 22:326–330.

Yasin M, Jeong Y, Park S, Jeong J, Lee EY, Lovitt RW, Kim BH, Lee J, Chang IS. 2015. Microbial synthesis gas utilization and ways to resolve kinetic and mass-transfer limitations. Bioresour Technol 177:361–374.